Biomedicine & Pharmacotherapy 158 (2023) 114192

Contents lists available at ScienceDirect

Biomedicine & Pharmacotherapy

journal homepage: www.elsevier.com/locate/biopha

Ginsenoside Rk3 ameliorates Aβ-induced neurotoxicity in APP/PS1 model mice via AMPK signaling pathway

Lingyu She [a,b,c,1], Li Xiong [b,c,1], Liwei Li [c], Jing Zhang [b], Jinfeng Sun [a,c], Haibin Wu [c], Juan Ren [d], Wei Wang [b,*], Xia Zhao [b,c,**], Guang Liang [a,b,c,***]

[a] Key Laboratory of Natural Medicines of the Changbai Mountain, Ministry of Education, Yanbian University, Yanji, Jilin 133002, China
[b] Affiliated Yongkang First People's Hospital, Hangzhou Medical College, Yongkang, Zhejiang 321399, China
[c] School of Pharmaceutical Sciences, Hangzhou Medical College, Hangzhou, Zhejiang 311399, China
[d] School of Laboratory Medicine and Bioengineer, Hangzhou Medical College, Hangzhou, Zhejiang 311399, China

ARTICLE INFO

Keywords:
Alzheimer's disease
Ginsenoside Rk3
Oxidative stress
APP/PS1
AMPK signaling pathway

ABSTRACT

Alzheimer's disease (AD) has become a major public health problem affecting the elderly population, and there is currently no effective treatment. Although the pathogenesis of AD is unclear, neurotoxicity induced by oxidative stress plays an important role in the progression of AD. Ginseng, the root and rhizome of *Panax ginseng* C. A. Meyer, is used not only as an herbal medicine but also as a functional food to support bodily functions. Ginsenoside Rk3 (Rk3), the main bioactive component in ginseng, has a strong antioxidant effect and has not been reported in AD. In this study, we showed that Rk3 improved neuronal apoptosis, decreased intracellular reactive oxygen species (ROS) production and restored mitochondrial membrane potential in PC12 and primary neuronal cells. In vivo, we found that Rk3 improved spatial learning and memory deficit in precursor protein (APP)/presenilin 1 (PS1) double transgenic mouse model of AD. Additionally, Rk3 increases glutathione reductase (GSH) and superoxide dismutase (SOD) levels while inhibits malondialdehyde (MDA) production, apoptosis and activation of glial cells in APP/PS1 mice. Mechanistically, we found that the protective effect of Rk3 is in correlation with the activation of AMPK/Nrf2 signaling pathway. In conclusion, the findings of this study provide support for Rk3 as a new strategy for the treatment of AD.

1. Introduction

Alzheimer's disease (AD), the most common form of dementia, has become one of the most serious society problems globally [1]. AD is characterized by intracellular neurofibrillary tangles (NFTs) and extracellular senile plaques [2]. Aβ is produced by cleavage of amyloid precursor protein (APP) by β-secretase and γ-secretase [3]. Studies have shown that soluble Aβ oligomers may be the most neurotoxic and pathological form in AD, impair synaptic function and memory and cognition, induce tau hyperphosphorylation; and stimulate the production of reactive oxygen species (ROS), which in turn cause oxidative stress [4].

Oxidative stress, as a key process in the mechanism of AD, is an important pathophysiological feature in the early stage of AD [5]. Oxidative stress participates in the development of AD by promoting Aβ deposition, tau hyperphosphorylation, and the subsequent loss of

Abbreviations: AD, Alzheimer's disease; APP, Amyloid precursor protein; APP/PS1, APPswe/PSEN1dE9; MDA, Malondialdehyde; GSH, glutathione reductase; SOD, superoxide dismutase; ROS, reactive oxygen species; RK3, Ginsenoside Rk3; BACE1, beta-site amyloid precursor protein cleaving enzyme protein 1; NFTs, neurofibrillary tangles; NOR, Novel object recognition; MWM, Morris water maze; TBA, thiobarbituric acid; HO-1, heme oxygenase 1; LDH, Lactate dehydrogenase; MAP2, Microtubule-associated protein 2; PSD95, Postsynaptic density protein 95; GFAP, Glial fibrillary acidic protein; TCM, Traditional Chinese medicine; Nrf2, nuclear factor erythroid-2-related factor 2; NQO1, NADPH: Quinone Oxidoreductase 1.

* Corresponding author.
** Corresponding author at: School of Pharmaceutical Sciences, Hangzhou Medical College, Hangzhou, Zhejiang 311399, China.
*** Corresponding authors at: Key Laboratory of Natural Medicines of the Changbai Mountain, Ministry of Education, Yanbian University, Yanji, Jilin 133002, China.
E-mail addresses: ykoneway@163.com (W. Wang), xiazhao@hmc.edu.cn (X. Zhao), wzmcliangguang@163.com (G. Liang).
[1] These authors contribute equally to this work.

https://doi.org/10.1016/j.biopha.2022.114192
Received 13 October 2022; Received in revised form 17 December 2022; Accepted 28 December 2022
Available online 30 December 2022

synapses and neurons [6]. The relationship between oxidative stress and AD suggests that oxidative stress is an essential part of the pathological process, and antioxidants may be useful for AD treatment. AMPK is an evolutionally conserved Ser/Thr kinase that serves a crucial physiological function as a cellular energy sensor [7]. Reduced energy metabolism due to oxidative stress is an early and consistent feature of AD [8]. For example, AMPK activation can improve brain energy metabolism and regulate amyloid precursor protein (APP) cleavage by inhibiting the expression of beta-site amyloid precursor protein cleaving enzyme protein 1 (BACE1), so as to reduce the production and accumulation of Aβ [9]. Notably, emerging evidence has revealed that boost of the AMPK signaling pathway could protect cells against oxidative injury by targeting Nrf2 signaling, indicating crosstalk between the AMPK and Nrf2 signaling pathways [10].

Due to the complex pathological features of AD, there is no effective treatment, so there is an urgent need to develop new therapeutic strategies. Single drug acting on single mechanism cannot achieve a good therapeutic effect. Therefore, the search for multi-target traditional Chinese medicine may be an effective strategy for the treatment of AD. The need to focus on effective complementary and functional foods to prevent and delay AD is increasing [11]. *Panax ginseng* C. A. Meyer is a natural herbal plant widely distributed in Asian countries, such as China, Korea, and Japan [12]. Ginseng, the roots and rhizomes of *P. ginseng* C. A. Meyer, is used not only in medicine but also as a functional food to support body functions. Recent studies have shown that ginseng extract, active ingredients ginsenosides (also called ginseng saponins) can improve symptoms and inhibit AD progression in AD patients by reducing Aβ deposition and tau hyperphosphorylation [13,14]. These effects may be mediated by mitochondrial function, neuronal conduction, apoptosis, calcium ions, and reactive oxygen species (ROS) [15–17]. Rk3 is a natural prebiotic found in ginseng, has excellent pharmacological efficacy, especially antitumor effects, and can greatly benefit human health [18]. Previous research has demonstrated that Rk3 has a strong protective effect on colitis, liver injury, and kidney injury [18,19], there is little research on the use of ginsenosides in AD or even neurodegenerative diseases.

In the present study, we explored the preventive and therapeutic potential and underlying mechanisms of ginsenoside Rk3 in in vitro and in vivo model of AD. Obtained results showed that ginsenoside Rk3 attenuate oxidative damage and AD-type pathologies via AMPK-Nrf2 signaling pathway. These findings provide a new therapeutic candidate for the treatment of AD.

2. Materials and methods

2.1. Reagents

Rk3 (95% purity, CAS: 364779–15–7) was obtained from Chengdu DeSiTe Biological Technology (DR0036–2), donepezil (95% purity, CAS: 110119–84–1) was obtained from Chengdu Alfa Biotechnology (AB1619), Aβ 1–42 (PA4391), Dulbecco's minimal essential medium (DMEM; D1152), 4, 6-diamidino-2-phenylindole (DAPI; C0065), 0.25% trypsin (BC-CE-005), DMSO (D2650), bovine serum albumin (BSA; A8020), Triton X-100 (P1080), 3-(4,5-dimethylthiazol-2-yl)− 2,5-diphenyl tetrazolium bromide (MTT; M2128), Reactive Oxygen Species Assay Kit(ROS; S0033) , 100 ×green streptomycin mixture (Double antibody; 15140–122), JC-1 (C2005), One Step TUNEL Apoptosis Assay Kit (TUNEL; C1086), a total superoxide dismutase assay kit (SOD; A001–3–2), and lipid peroxidation malonaldehyde assay kit(MDA; A00–1–2), Glutathione assay kit(GSH; A006–2–1), Annexin V-FITC/PI Apoptosis Detection Kit (abs50001), AMPK inhibitor (Compound C, HY-13418A), ™Neurobasal Medium(21103049), Gibco™ B-27™ Additive (17504044), PVDF membrane (SEQ00010), Immobilon Western Chemiluminescent HRP substrate (FD8030), Mouse Aβ42 ELISA Kit (Fine Test, EM0864), Mouse Aβ40 ELISA Kit (Fine Test, EM0863), Mouse Soluble Amylase Precursor Protein (SAPPβ) ELISA Kit(Shanghai Yanqi Biotechnology, YQ-3360), Mouse p-Tau ELISA Kit(Shanghai Yanqi Biotechnology, YQ-2936) and Mouse Tau ELISA Kit(PYRAM, PM104488). All antibodies used in this work are listed in Table S1. List of primer used in this study is presented in Table S2.

2.2. Cell Culture

Rat pheochromocytoma cells (PC12 cells) (SNL-124) culture: PC12 cells were cultured in high-glucose Dulbecco's modified Eagle's medium, supplemented with 10% FBS, 100 μg/ml streptomycin, and 100 units/ml penicillin and maintained at 37 °C in a humidified atmosphere of 5% CO2. The medium was changed every 3–4 days, and the cell cultures were propagated to new flasks once a week. The cells were grown up to 70–90% confluency for experimental purposes.

Hippocampal Neurons Culture: Newborn C57BL/6 mice were procured from the animal facility of Hangzhou Medical College. The whole body was disinfected with 75% alcohol and the brain was surgically removed and stored into cold PBS. The whole hippocampus region was dissected using a glass rod which was bent on both sides. The hippocampus was cleared of blood and mixed vessels by washing three times with DMEM high glucose medium. Then the hippocampus was chopped into 1 mm pieces using scissors was digested with 0.125% of trypsin at 37 °C for 20 min. Shake gently every five minutes. The enzymatic digestion was stopped with 10% FBS and DMEM high glucose medium was added to the digested hippocampus tissue in a 50 ml centrifuge tube. Pass the turbid tissue supernatant through a 40 μM cell strainer in another 50 ml centrifuge tube. Centrifuged at 1000 rpm for 10 min. The resulting cell pellet was resuspended in Neurobasal with B27 and incubated for growth at 37 °C in 5% CO2 humidified atmosphere.

2.3. Aβ oligomer preparation

β-amyloid is the main extracellular component of AD plaques, has strong neurotoxic effects, and is the main cause of neuronal degeneration and death in senile plaques of AD patients [20,21]. Soluble Aβ1–42 oligomers are thought to be the major component and are often used in in vitro models. In this study, Aβ1–42 stock solution was prepared in sterile Dimethylsulfoxide at a concentration of 10 μM, and the aliquots were stored at − 20 °C. As previously mentioned, Aβ1–42 was allowed to aggregate by incubation at 37 °C for 7 days before use [22–24]. When performing experiments, Aβ1–42 was further diluted to 10 μM in culture medium.

2.4. Animal and drug administration

APP/PS1 mice (APPswe, PSEN1dE9) were obtained from the Jackson Laboratory and bred in the animal facility of Hangzhou Medical College. Mice were housed 3–4 per cage, with free access to food and water, under standard specific-pathogen-free laboratory conditions. The APP/PS1 mice (8 months old, male n = 7, weight 30–32 g) were randomly divided into five groups: Wild-type (WT), APPswe/PS1dE9 double transgenic mice (APP/PS1), APP/PS1 treated with 1 mg/kg Rk3(APP/PS1 +1 mg/kg Rk3), APP/PS1 treated with 10 mg/kg Rk3(APP/PS1 +10 mg/kg Rk3) [25] and APP/PS1 treated with 5 mg/kg donepezil (APP/PS1 + 5 mg/kg donepezil) [26]. All drugs were dissolved in 2% DMSO in PBS, and the control group was given an equal volume of 1xPBS (containing 2% DMSO). Before administering the drug, the mice in each group were weighed and administered intraperitoneally according to their body weight. All groups were injected intraperitoneally once a day for one month.

2.5. Novel object recognition (NOR)

To evaluate the recognition memory of the mice, the NOR test was performed. Briefly, two identical circular objects were placed in the arena (50 cm long x 50 cm wide x 40 cm high), on the first day, each

mouse was given 5 min to explore the objects. The next day, a round object was swapped out for a square one, and each mouse still had 5 min to explore these square novel object. Exploratory behavior was defined as when the mice pointed its nose at an object within 2 cm and/or made direct contact with the object with its nose and/or front paws. The discrimination index is calculated as the time spent exploring novel object and the number of explorations. The principle of the NOR test is that mice have the desire to detect novel objects. If cognitive function is unobstructed, it takes longer to explore novel objects.

2.6. Morris water maze (MWM)

To investigate spatial learning and memory in mice, the Morris water maze (MWM) test was performed. The test involves a 6-day test. Mouse were allowed to swim in the tank. Mice were previously trained for 1 day to feel a platform in the tank. The mouse then underwent a navigation test in which they searched for a hidden platform 1 cm underwater for 5 days. Three tests were performed on the mice, each lasting up to 60 s with 60-second intervals. Escape latency was recorded using an overhead video tracking system. Finally on day 7, the platform was removed from the tank and a probe test was performed to assess the mice's search bias.

2.7. Preparation of tissue samples

After the behavioral tests, all mice were euthanized using chloral hydrate (0.25 mg/ml), After transcranial perfusion with precooled 0.9% saline, the animals were sacrificed by decapitation. The mice brains were sagittal cut in half. And the brains were dissected and fixed in 4% paraformaldehyde (4% PFA) for 24 h at 4 ℃. After fixation, some of the samples were dehydrated and embedded in OCT, and kept at − 80 °C until further analysis.

2.8. Immunofluorescent staining (IF)

Sections were incubated with the following primary antibody at 4 °C overnight , followed by appropriate Alexa-Fluor-conjugated secondary antibody at RT for 1 h. Sections were mounted with slow fade® anti-fade DAPI reagent. The images were acquired with a Nikon A1 confocal microscope. All studies were performed three times.

2.9. Western blot assays

Protein was extracted from cells or tissue homogenates using RIPA buffer supplemented with a protease phosphatase inhibitor cocktail. The protein concentration was measured using a BCA protein assay kit. Twenty-microgram of protein was loaded on sodium dodecyl sulfate polyacrylamide gels to separate the proteins. The separated proteins were then transferred onto polyvinylidene fluoride (PVDF) membranes, which were probed with the primary antibodies listed in Supplementary Table S1. After being rinsed, the PVDF membranes were incubated with appropriate HRP-conjugated secondary antibodies. The immunoreactive bands were visualized with an enhanced chemiluminescence kit. The intensity of the bands was quantified using Image J software.

2.10. SOD, MDA and GSH assay

The assays were performed according to the instructions provided by the manufacturer. A total SOD assay kit, a lipid peroxidation MDA assay kit and GSH assay kit (Beyotime Institute of Biotechnology, Shanghai, China) were used to measure SOD and MDA contents, respectively. Briefly, SOD activity was determined by WST-8 method. WST-8 can react with the superoxide anion catalyzed by xanthine oxidase to produce water-soluble formazan dye which can be measured at a wavelength of 450 nm. MDA content was determined on a color reaction based on the reaction of MDA and thiobarbituric acid (TBA) to produce a red product which can be measured at a wavelength of 532 nm. Glutathione reductase can reduce oxidized glutathione (GSSG) to GSH, and GSH can react with the chromogenic substrate DTNB to produce yellow TNB and GSSG, and can be determined by A412 to detect the production of TNB. Absorbances were measured using a BIO-RAD680 microplate reader (Thermo Fisher, MA, USA).

2.11. MTT assay

The cell viability was assessed using MTT assay as previously described. Cells were seeded in 96-well plates at a density of 1 × 104 cells/well in complete medium. After appropriate the treatment, cells were further incubated with MTT (0.5 mg/ml) for additional 3 h, and the medium was replaced with 100 μL DMSO to dissolve the blue formazan crystals formed by live cells. The absorbance was measured at 570 nm using a microplate reader (SpectraMax 250, Molecular Device, Sunnyvale, CA, USA). Cell viability was calculated as a percentage of the control group.

2.12. TUNEL assay

TUNEL staining was used to test cellular apoptosis, according to the instructions provided by the manufacturer (C1090, Beyotime, Shanghai, China). TUNEL-positive cells (green fluorescence) were observed under a fluorescent microscope and counted. The apoptosis was calculated as a percentage of the total number of cells. For tissue samples the same methodology was used.

2.13. Flow cytometry

PC12 cells (5 ×105 cells/well) were seeded into 12-well plates. After appropriate treatment the cells were harvested and centrifuged at 1000 rpm for 5 min. The cells were rinsed twice with ice-cold PBS and resuspended in Annexin V-FITC/PI binding buffer (195 μL). Annexin V-FITC (5 μL) was added and the cells were kept in the dark at room temperature for 30 min. Cells were then centrifuged at 1000 rpm for 5 min and re-suspended in Annexin V-FITC/PI binding buffer (190 μL). Propidium iodide (PI) (10 μL) was further added and allowed to incubate in the dark for 5 mins. The quantification of apoptotic cells was performed using flow cytometry analysis.

2.14. Measurement of reactive oxygen species (ROS)

The levels of intracellular ROS were tested using the fluorescent probe DCFH-DA (Beyotime, S0033S, China). After appropriate treatment, according to the protocol provided by the manufacturer. The fluorescence was measured with an Infinite M200 PRO Multimode Microplate using 488 nm excitation wavelength, 525 nm emission wavelength.

2.15. Measurement of mitochondrial membrane potential (△ψm)

The mitochondrial membrane potential (△ψm) was measured by mitochondrial membrane potential assay kit with JC-1(Beyotime, C2006, China), according to the protocol provided by the manufacturer. After appropriate treatment, the cells were incubated with 1x JC-1 (10 μg/ml in medium without FBS) at 37 °C for 30 min and washed two times with PBS solution. The intensities of red fluorescence (excitation 560 nm, emission 595 nm) and green fluorescence (excitation 485 nm, emission 535 nm) were measured using an Infinite M200 PRO Multimode Microplate. The ratio of JC-1 red/green fluorescence intensity was used to calculate the △ψm. All the values were normalized to the control group.

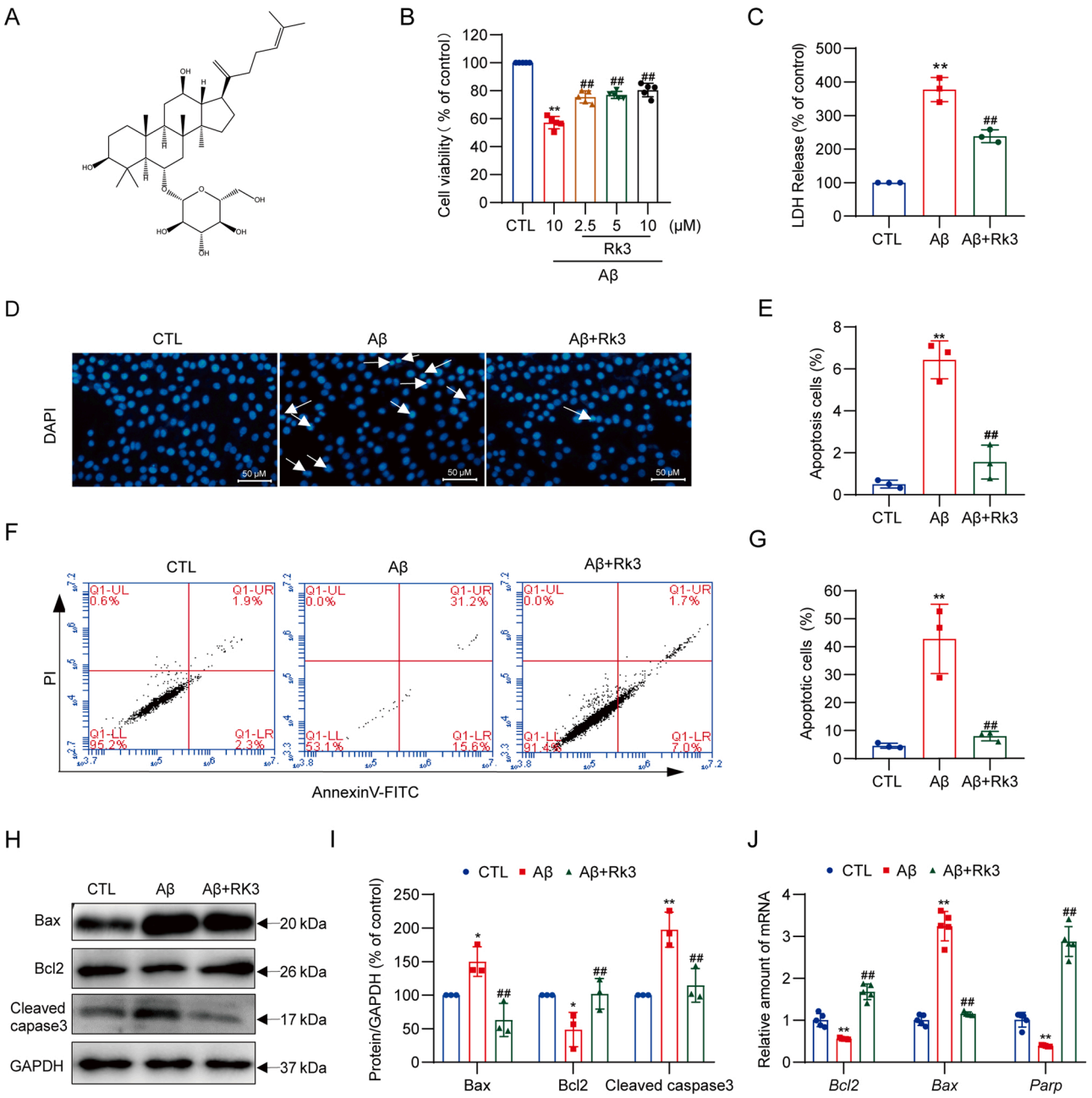

Fig. 1. Rk3 decreased Aβ-induced apoptosis in PC12 Cells. (A) Chemical structure of Ginsenoside Rk3. (B) Rk3 attenuated the decrease in cell viability caused by Aβ1–42 in PC12 cells. PC12 cells were grown in 96-well plates and pretreated with Ginsenoside Rk3 at indicated concentrations and then induced with or without 10 μM Aβ for a further 24 h and cell viability was measured using the MTT assay. (C-J) Cells were pretreated with 10 μM Rk3 for 24 h and then induced with or without 10 μM Aβ1–42 for a further 24 h. (C) Cell viability was measured by LDH release assay. (D)Apoptotic cells were observed by DAPI staining as shown in fluorescence images taken with a fluorescence microscope. The apoptotic cells with condensed chromatin are indicated by an arrowhead. (E) Quantitation of (D) apoptotic cell's nuclei. (F) Apoptosis was determined by flow cytometry. Photographs of representative cultures measured. (G) Quantitative analysis of (F). (H) Western blot analysis of Bax, cleaved caspase-3 and Bcl-2 in PC12 cells. GAPDH was used as the loading control. (I) Quantitative data of the blot intensity of corresponding proteins were determined by Image J software in-plane A. (J) RT-qPCR showing mRNA levels of Bax, Bcl-2, and Parp in the PC12 cells. Results are presented as mean ± SEM (n = 3). *P < 0.05 or * *P < 0.01, or * **P < 0.001, CTL vs Aβ1–42; $^{\#}$P < 0.05 or $^{\#\#}$P < 0.01 Aβ vs Aβ+ Rk3·

2.16. Statistical analysis

Statistical analysis was performed using GraphPad Prism 8 software. All results are expressed as the mean ± SEM from three experiments. The statistical significance between multiple groups was determined using one or two-way ANOVA followed by Tukey's post-hoc test. p < 0.05 was considered statistically significant.

3. Results

3.1. Rk3 decreased Aβ-induced apoptosis in PC12 Cells

To test the protective effects of Rk3(Fig. 1 A), PC12 cells were pre-treated with Rk3 for 24 h before being exposed to Aβ for another 24 h. This result showed that pre-treatment with Rk3 significantly reduced Aβ-induced cell death (Fig. 1B). Similarly, Rk3 treatment reduced Aβ-induced LDH release (Fig. 1 C). To further investigate the

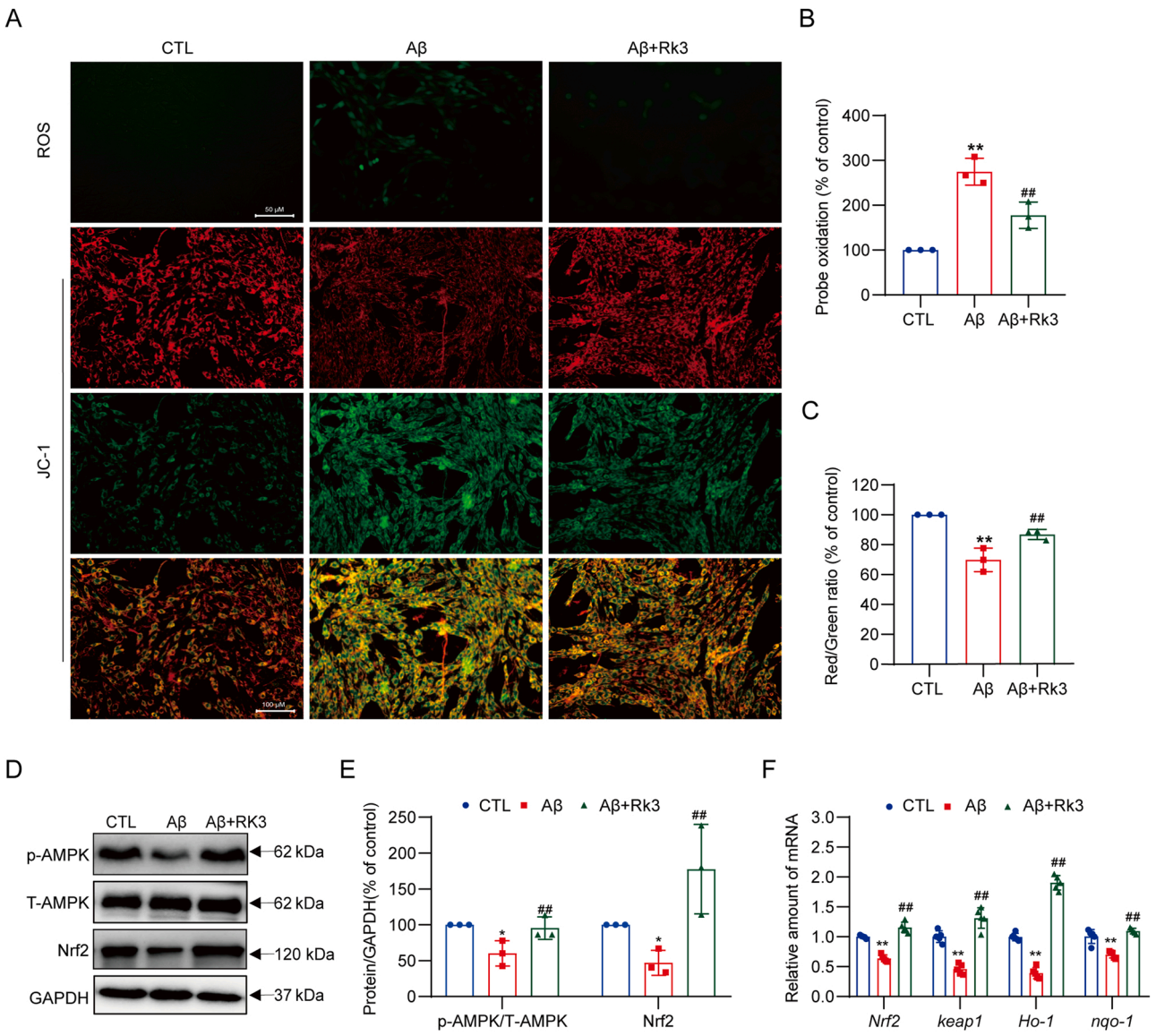

Fig. 2. Rk3 reduced Aβ-induced intracellular ROS level and restored mitochondrial membrane potential via AMPK activation in PC12 cells. PC12 cells pretreated for 24 h with 10 μM Rk3 followed by exposure for 24 h with 10 μM Aβ. (A) The fluorescent images represent the ROS level as determined by the probes DCFH-DA and by staining the cells with JC-1 dyes. (B) Quantitation of the percentage of the cellular ROS level. (C) Red to green fluorescence intensity ratio (increase of mitochondrial membrane potential). (D) Expression of p-AMPK; T-AMPK and Nrf2 were detected by using Western blot. (E) Quantification of p-AMPK; T-AMPK and Nrf2. (E) RT-qPCR showing mRNA levels of Nrf2, keap1, Ho1 and Nqo1 in the PC12 cells. Results are presented as mean ± SEM (n = 3). * $P < 0.05$ or * *P < 0.01, or * **P < 0.001, CTL vs Aβ1–42; $^{\#}P < 0.05$ or $^{\#\#}P < 0.01$ Aβ vs Aβ+ Rk3.

neuroprotective effect of Rk3 on Aβ-induced apoptosis. Nuclei condensation was observed in PC12 cells after exposure to 10 μM Aβ while pretreatment with 10 μM Rk3 significantly improved these changes (Fig. 1D-1E) (arrowheads). The result was further confirmed using flow cytometry for Annexin V-FITC/PI-positive cells and data from these experiments indicated that Aβ exposure markedly increased apoptosis in PC12 cells, while 10 μM Rk3 pretreatment significantly reduced the apoptosis caused by Aβ (Fig. 1F-1 G). In addition, our data showed that Aβ-induced PC12 cells significantly increased the level of pro-apoptotic Bax and suppressed the level of anti-apoptotic Bcl-2 in the PC12 cell, whereas Rk3 pretreatment for 24 h reversed these changes (Fig. 1H-1I). The mRNA levels of Bax and Bcl-2 measured by RT-qPCR were consistent with the protein levels (Fig. 1 J). Apoptotic data was also confirmed by immunoblotting for cleaved caspase-3, which showed that Rk3 significantly reduced the Aβ-induced increase in cleaved caspase-3 in PC12 cells (Fig. 1H-1I). PARP, a substrate of caspase-3, is considered to be an important indicator of apoptosis. According to the results of RT-qPCR experiments, Rk3 significantly increased the Aβ-induced decrease in the mRNA expression level of PARP in PC12 cells.

3.2. *Rk3 reduced Aβ-induced intracellular ROS level and restored mitochondrial membrane potential via AMPK activation in PC12 cells*

The above result demonstrated that Rk3 can protect Aβ-induced apoptosis, whereas oxidative stress has been thought to trigger and sustain the pathogenesis of Aβ-induced damage. We examined the effects of Rk3 on oxidative stress by determining the contents of ROS. We investigated whether Rk3 blocked Aβ-induced oxidative stress in PC12 cells. Cellular oxidative stress was determined by the fluorescence probes DCFH-DA. As expected, (Fig. 2A-2B), Aβ-induced an increase in intracellular ROS content compared to the control cells. The pretreatment with Rk3 attenuated the high ROS level induced by Aβ. Thus, Rk3 was capable of attenuating intracellular ROS production, suggesting that Rk3 may be a potent scavenger of free radicals. The mitochondria could

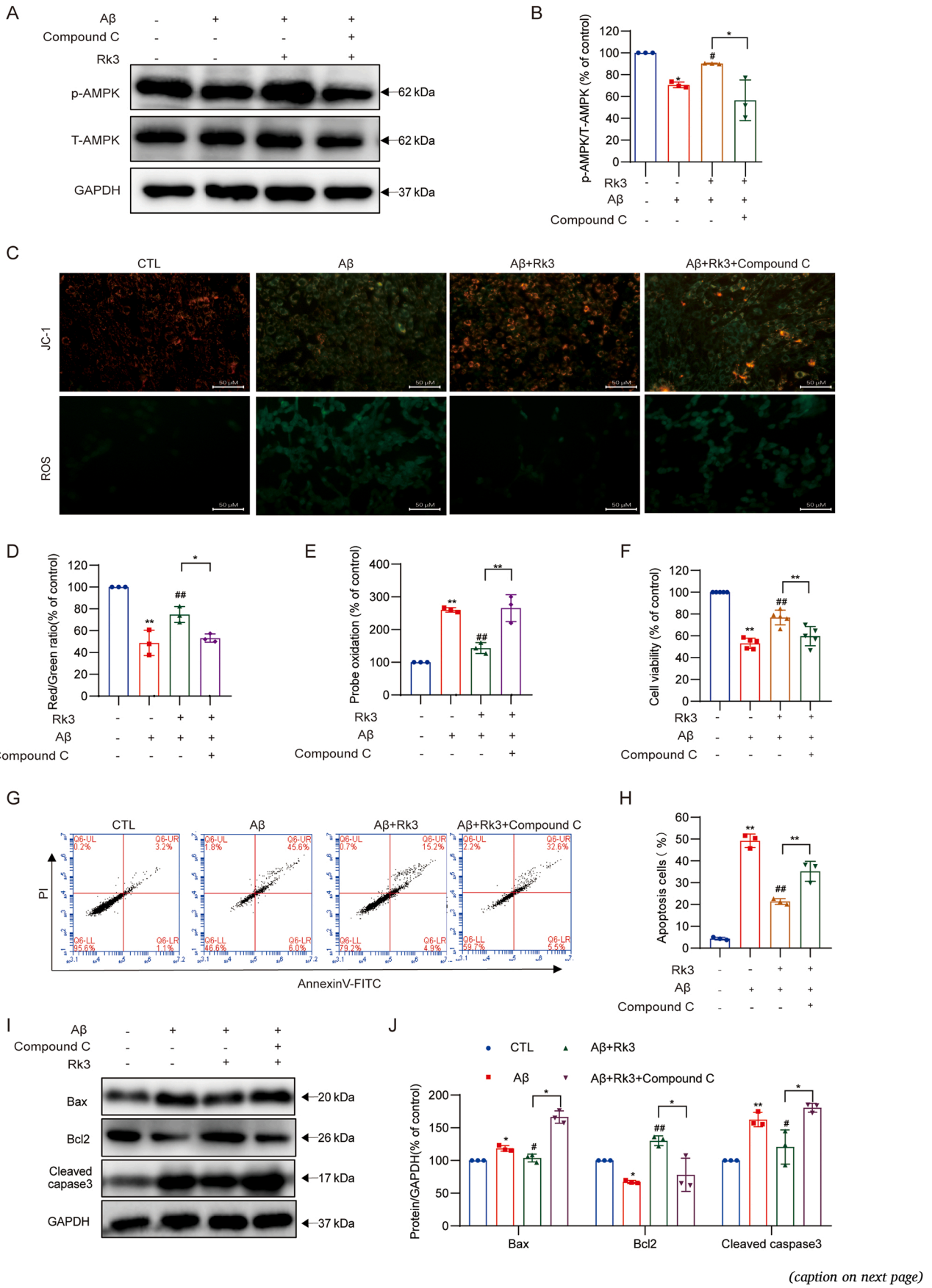

(caption on next page)

Fig. 3. Protective effects of Ginsenoside Rk3 in PC12 cells was reversed by AMPK inhibitor. PC12 cells were pretreated with or without the presence of 2 μM compound C. After 30 min, PC12 cells are used 10 μM Rk3 for 24 h. Then, cells were exposed to 10 μM Aβ for 24 h. (A) Western blot analysis of p-AMPK and T-AMPK in PC12 cells. (B) Quantitative data of the blot intensity of corresponding proteins were determined by Image J software in-plane A. (C) The fluorescent images represent the ROS level as determined by the probes DCFH-DA and by staining the cells with JC-1 dyes. (D) Quantitation of the percentage of the cellular ROS level. (E) Red to green fluorescence intensity ratio (increase of mitochondrial membrane potential). (F) Cell viability was measured using the MTT. (G) Representative flow cytometry images. (H) Quantitation of the percentage of cell apoptosis. (I) Western blot analysis of Bax, Cleaved caspase-3 and Bcl2 in PC12 cells. GAPDH was used as the loading control. (J) Quantitative data of the blot intensity of corresponding proteins were determined by Image J software in-plane A. Results are presented as mean ± SEM (n = 3). Results are presented as mean ± SEM (n = 3). * $P < 0.05$ or * *P < 0.01, or * **P < 0.001, CTL vs Aβ1–42; $^{\#}$P < 0.05 or $^{\#\#}$P < 0.01 Aβ vs Aβ+ Rk3.

be the origin of the observed ROS production and Mitochondrial damage can directly cause formation of oxidative stress, as well as mechanism of apoptosis. To evaluate the mitochondrial function, mitochondrial membrane potential (△ψ m) was detected using JC-1 probe. Compared with the control, after Aβ-induced red/green fluorescence ratio was reduced to 50%. However, this reduction was reversed by pretreatment with Rk3 (Fig. 2C-2D). Next, to explore the molecular mechanism underlying the effects of Rk3 against Aβ, the redox-related signaling pathways were analyzed. AMPK is a major regulator of mitochondria energy homeostasis, plays an important role in oxidative stress, and involves in the pathogenesis of AD [27]. Studies have shown that ginsenosides can mediated the activation of AMPK [28]. Therefore, we tested whether Rk3 is involved in Aβ-induced neurotoxicity through AMPK. As expected, the phosphorylation of AMPK was decreased by 30–60% after Aβ treatment, compared with the control. Rk3 pretreatment 24 h of Aβ-Induced treated PC12 cell cultures changed the phosphorylation of AMPK which were significantly increased, closed to phosphorylation values in control untreated cultures (Fig. 2E-2 F). Nrf2 has been identified as one of the main transcription factors associated with the oxidative stress response [29]. Several previous studies have testified that Nrf2 and its downstream protein like heme oxygenase 1 (HO-1) and NAD(P)H:quinone oxidoreductase 1 (NQO1) could be enhanced by the activation of upstream AMPK [30]. Western blotting results showed that the levels of Nrf2 were reduced by treatment with Aβ. Remarkably, pretreatment with Rk3 increased Nrf2 compared to Aβ-Induced cells (Fig. 2E-2 F). The mRNA levels of Nrf2; HO-1 and NQO1 measured by RT-qPCR were consistent with the protein levels (Fig. 2 G). Nrf2 activity is precisely regulated by Kelch-like-ECH-associated protein 1 (Keap1). Therefore, we tested the mRNA expression level of Keap1. Results showed that keap1 was reduced by treatment with Aβ. Whereas pretreatment with Rk3 increased keap1 compared to Aβ-Induced cells (Fig. 2E-2 F).

3.3. Protective Effects of Rk3 in PC12 Cells were reversed by AMPK inhibitor

Compound C (also called dorsomorphin), a cell-permeable, potent, relative selective, and reversible ATP-competitive inhibitor of AMPK, has been widely used in cell-based, biochemical, and in vivo assays as an AMPK inhibitor. To further evaluate whether AMPK was responsible for the anti-oxidative stress effect of Rk3 on Aβ-induced PC12 cells, PC12 cells were pretreated with or without Compound C, before the addition of Rk3 and Aβ. Pretreatment with Compound C exhibited obvious conversion effects of Rk3 on p-AMPK (Fig. 3A-3B). Subsequent JC-1 and ROS experiments showed that Compound C pretreatment reversed the protective effect of Rk3 against oxidative stress (Fig. 3C-3E). Next cell viability was measured by MTT assay (Fig. 3 F), cell apoptosis was measured by Annexin-V-FITC FACS assay (Fig. 3G-3 H) in parallel with measurements of apoptosis indicator Bax; Bcl-2 and cleaved caspase3 expression level (Fig. 3I-3 J). These results indicated that Compound C reversed the protective effect of Rk3 on apoptosis. Together, these data suggest that Rk3 inhibits Aβ-induced neurotoxicity via the AMPK signaling pathway in PC12 cells.

3.4. Rk3 improved learning and memory in APP/PS1 mice

APP/PS1 is a particularly aggressive transgenic mouse model generated by mutant transgenes of APP (APPswe: KM594/5NL) and PS1 (dE9: exon 9 deletion). Both mutations are associated with early-onset AD. Widely used to study the biochemical and pathological mechanisms of AD and to explore therapeutic approaches [31]. The way of drug administration is shown in (Fig. 4 A), and the experimental flow of novel object recognition is shown in Fig. 4B. The desire to explore things on the first day of APP/PS1 was significantly lower than that of the WT group, but it was significantly improved after administration (Fig. 4C-E). It shows that the cognitive function of mice is significantly improved after administration with Rk3. After changing to a new object on the second day, it can be seen from the number of touches and the exploration time of the new object that the short-term memory ability of the mice in the APP/PS1 group was significantly decreased, and the short-term memory ability of the mice was improved after administration, and the number of touches significantly higher than that in the donepezil group (Fig. 4 C and Fig. 4F-4 G). RK3 treatment significantly improved spatial learning in APP/PS1 mice by shortening escape latency during hidden platform testing, and this improvement was significantly better than donepezil group at day 5 (Fig. 4H and Fig. 4 J). Rk3 also increased the frequency without altering total distances during the probe trial (Fig. 4I and Fig. 4K-4 L) in the MWM test.

3.5. Rk3 treatment reduced AD pathology in APP/PS1 mice brains

There is a good consensus that synaptic function is a pathological feature closely related to the learning and memory abilities of AD. To examine whether synaptic plasticity impairment is attenuated after rk3 administration, we analyzed the protein levels of PSD95 (a postsynaptic density protein) and MAP2 (microtubule-binding protein 2). As the picture shows (Fig. 5,A-5 C), Rk3 treatment alleviated the decrease in the levels of these proteins in APP/PS1 mice better than donepezil group. In addition, Rk3 administration rescued the impaired synaptic plasticity in APP/PS1 transgenic mice, and the effect was better than that of donepezil.

Extracellular amyloid plaques and intracellular NFTs are known to be hallmarks of AD [32]. To further evaluate the therapeutic effect of Rk3 on these pathological hall markers, we performed immunofluorescence. As shown in Fig. 5D, Rk3 or donepezil treatment significantly reduced Aβ plaques in the brains of APP/PS1 mice. We next analyzed the levels of Aβ42, Aβ40 and soluble APPβ (sAPPβ) in mouse hippocampal lysates by ELISA and found that RK3 administration significantly reduced the levels of Aβ42, Aβ40 and sAPPβ in APP/PS1 mice, suggesting that RK3 can reduce the production of toxic Aβ by affecting the cleavage of APP (Fig. 5E-5 G). Quantitative analysis of western blot confirmed the qualitative histological findings (Fig. 5I-5 J). Then, we linked the Aβ1–42 used in this manuscript to the FITC label and found that the fluorescence intensity of the Rk3 treatment group significantly decreased, indicating that Rk3 has an inhibitory effect on the aggregation of Aβ (Fig. S1). Similarly, tau hyperphosphorylation was increased in APP/PS1 mice, and tau hyperphosphorylation was decreased after Rk3 treatment. To further confirm our result, the amount of total tau and p-Tau has been measured by ELISA, and the quantification of P-Tau and Tau showed that Rk3 treatment significantly reduced tau

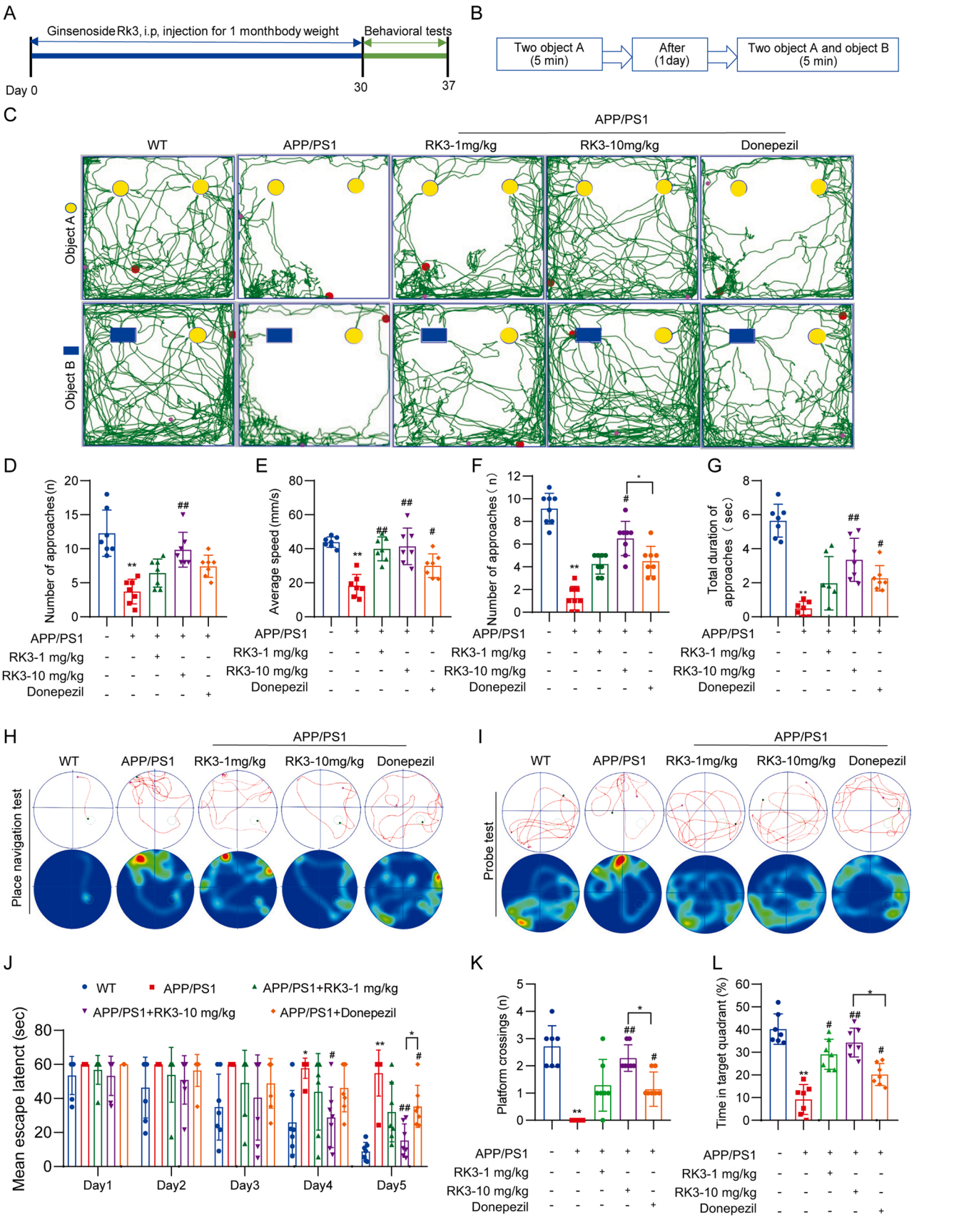

(caption on next page)

Fig. 4. Rk3 improved learning and memory in APP/PS1 mice 8–month-old APP/PS1 mice were administered Ginsenoside Rk3 by intraperitoneal injection once a day. (B) Flow chart of novel NOR test. (C) Representative novel object recognition experiment images. (D) Preference for things on the first day of the new object recognition test. (E) Average speed on the first day of the new object recognition test. (F) Number of new object approaches of the new object recognition test. (G) Number of new object approaches of the new object recognition test. (H) The representative swimming trace in probe trial of morris water maze test on day 5. (I) The representative swimming trace in probe trial without hidden platform of morris water maze test on day 6. (J) The escape latency results from the Morris water maze test on days 1–5. (K) The average crossing platform times of each group mice within 60 s in day 6. (E) Time spent in the target quadrant where the platform had been located in day 6. Data are presented as mean ± SEM of n = 7 mice per group. *P < 0.05 or * *P < 0.01, or * **P < 0.001 versus the WT group; $^{\#}$P < 0.05 or $^{\#\#}$P < 0.01 versus the APP/PS1 group.

hyperphosphorylation (Fig. 5H). To further confirm our result, we checked phosphorylation of tau using western blot. As expected, Rk3 also decreased the expression of P-Tau (Fig. 5H-5 K).

Inflammation is another important pathophysiological feature of AD, accompanied by the activation of glial cells and the release of inflammatory factors. Glial fibrillary acidic protein (GFAP) is the major intermediate filament protein that constitutes the astrocytic cytoskeleton [33]. Increased GFAP expression induces reactive gliosis and brain injury and deterioration [34]. Microglia are critical in the progression of AD by mediating neuroinflammatory responses [35]. To further determine the effect of Rk3 on inflammation, we analyzed the expression of microglia and astrocytes by immunofluorescence staining and western blot. Obtained results showed that Rk3 administration significantly reduced the activation of microglia and astrocytes in mice hippocampus and cortex. (Fig. 6 A). Similar results were obtained by western blot analysis of Iba1 and GFAP (Fig. 6B-6 C).

3.6. Rk3 attenuated the histopathological changes and decreased neuronal apoptosis in App/PS1 mice by activation of AMPK

In order to verify the effect of Rk3 on apoptosis in the mouse hippocampus, the protein expressions of Bax, Bcl-2 and cleaved caspase3 were analyzed by western blotting (Figure7A-7 C). The Rk3 high-dose group significantly increased the expression of Bcl-2/Bax in the APP/PS1 group, and the effect was better than that in the donepezil group. In addition, Rk3 treatment significantly inhibited the increase in the expression of cleaved caspase3 in the hippocampus of APP/PS1 mice, suggesting Rk3 have a good anti-apoptosis effect. To further confirm this, we used immunofluorescence to label neurons in the CA1, DG, and cortex of the hippocampus with a NeuN antibody, and analyzed the number of neurons. Results found that compared with the WT group, neurons in the APP/PS1 group were significantly reduced, and the Rk3 high-dose group reversed this reduction in different brain regions (Fig. 7D-7 G).

Oxidative stress is an early event in AD pathogenesis and can precede the formation of Aβ deposits [36]. Therefore, by-products of oxidative biomolecular damage such as MDA, SOD and GSH were quantitatively analyzed, is widely used to assess oxidative stress. The results shown in Fig. 8A-8 C indicate that MDA levels, SOD and GSH activity were significantly affected in APP/PS1 mice compared to previously reported wild-type mice. These changes were significantly altered by high-dose RK3 treatment, and these findings further support the proposal that the antioxidant effect of Rk3 is associated with inhibition of cerebral cortical apoptosis and attenuated cognitive deficits in the 3xTg mouse model. Next, since the protective effect of Rk3 on PC12 cells is through the activation of AMPK, we explored whether the activation of the AMPK/Nrf2 pathway could be detected in the hippocampus of Rk3-treated APP/PS1 mice. Consistent (Fig. 8D-8E), Rk3 treatment activated the AMPK/Nrf2 pathway. Therefore, it is concluded that the antioxidant effect of Rk3 is through the AMPK/Nrf2 pathway.

3.7. Rk3 protected primary cultured hippocampal neurons against Aβ-induced injury via AMPK kinase

To further verify the protective effect of Rk3, whether through AMPK, we also tested whether the protective effect of Rk3 on Aβ-induced primary neurons was reversed by Compound C, Mitochondrial membrane potential (Δψm) and intracellular ROS were both obtained and PC12 cells The results were consistent with those above (Fig. 9A-9 C). TdT-mediated dUTP nick end labeling (TUNEL) staining showed (Fig. 9A-9D) that Rk3 treatment reduced Aβ-induced apoptosis in primary neurons, which protected the effect was reversed by Compound C, which was further confirmed by MTT experiments (Fig. 9E). Therefore, the above experiments can indicate that Rk3 has a protective effect on Aβ-induced primary neuron damage through the AMPK pathway.

2. Discussion

In the present work, we demonstrated for the first time that RK3 has an effective therapeutic effect on AD. Suggest that Rk3 is a potential AD therapeutic. Our research shows that Rk3 can reduce Aβ-induced apoptosis, intracellular ROS levels, restore mitochondrial membrane potential in PC12 and primary cultured neurons. We further explored the protective effects of Rk3 by activating the AMPK/Nrf2 pathway, and these protective effects were reversed by AMPK inhibitor (Compound C). Similarly, APP/PS1 mice model results showed that Rk3 improved cognitive deficits and AD-type pathology in correlation with the activation of AMPK/Nrf2, and Rk3 was significantly higher than donepezil in improvement of pathological features of cognition and apoptosis. Taken together, these studies have identified a new potential drug candidate for the treatment of AD.

AD is a chronic, multifaceted and multifactorial neurodegenerative disease [37]. Due to the multiple pathological characteristics of AD, the current one-molecule-one-target strategy therapy fails to address the problem of AD. Traditional Chinese medicine (TCM) synergism often found in TCM preparation were found effective to combat disease heterogeneity as found in complex pathogenesis of AD [38]. Ginseng is a typical medicinal and edible herb, and studies have shown that ginseng can be supplied by medicinal materials and dietary sources [39]. Different bases, multi-targets alleviate AD and AD complications. Ginsenosides are mainly classified into protopanaxadiol (PPD) and protopanaxatriol (PPT), and according to their sapogenins, can significantly improve AD symptoms. As the main ginsenosides in ginseng, Rb1, Rb2, Re, Rd and Rc inhibit the activity of β-secretase [17]. It will eventually reduce the production of Aβ [40,41]. Ginsenosides Rg1, Rh2 are also involved in the APP regulatory pathway [42–44]. The indirect regulation of tau hyperphosphorylation by ginsenoside Rd has also been reported [45]. Ginsenoside Rk3, as one of the major rare saponins in heat-treated ginseng, plays a variety of biological roles, including anti-apoptotic, inhibition of inflammation, oxidative stress [46]. Previous studies have found that Rk3 has strong AChE inhibitory activity [47], but its real therapeutic effect on AD remains unclear. In this study, we found that RK3 can reduce the neurotoxicity of Aβ to neuronal cells and improve the learning and memory ability of AD.

Excessive accumulation of ROS has been recognized as an important marker of Aβ neurotoxicity, and Aβ exposure resulted in increased ROS release in cultured PC12 cells which leads to cell necrosis and apoptosis [5]. To combat oxidative stress, activation of endogenous antioxidant defense systems is required, the antioxidant defense system includes several enzymes and small molecules, such as heme oxygenase-1(HO-1), superoxide dismutase (SOD) enzymes, glutathione (GSH), catalase (CAT), thioredoxin (Trx) proteins, thioredoxin reductase (TrxR)

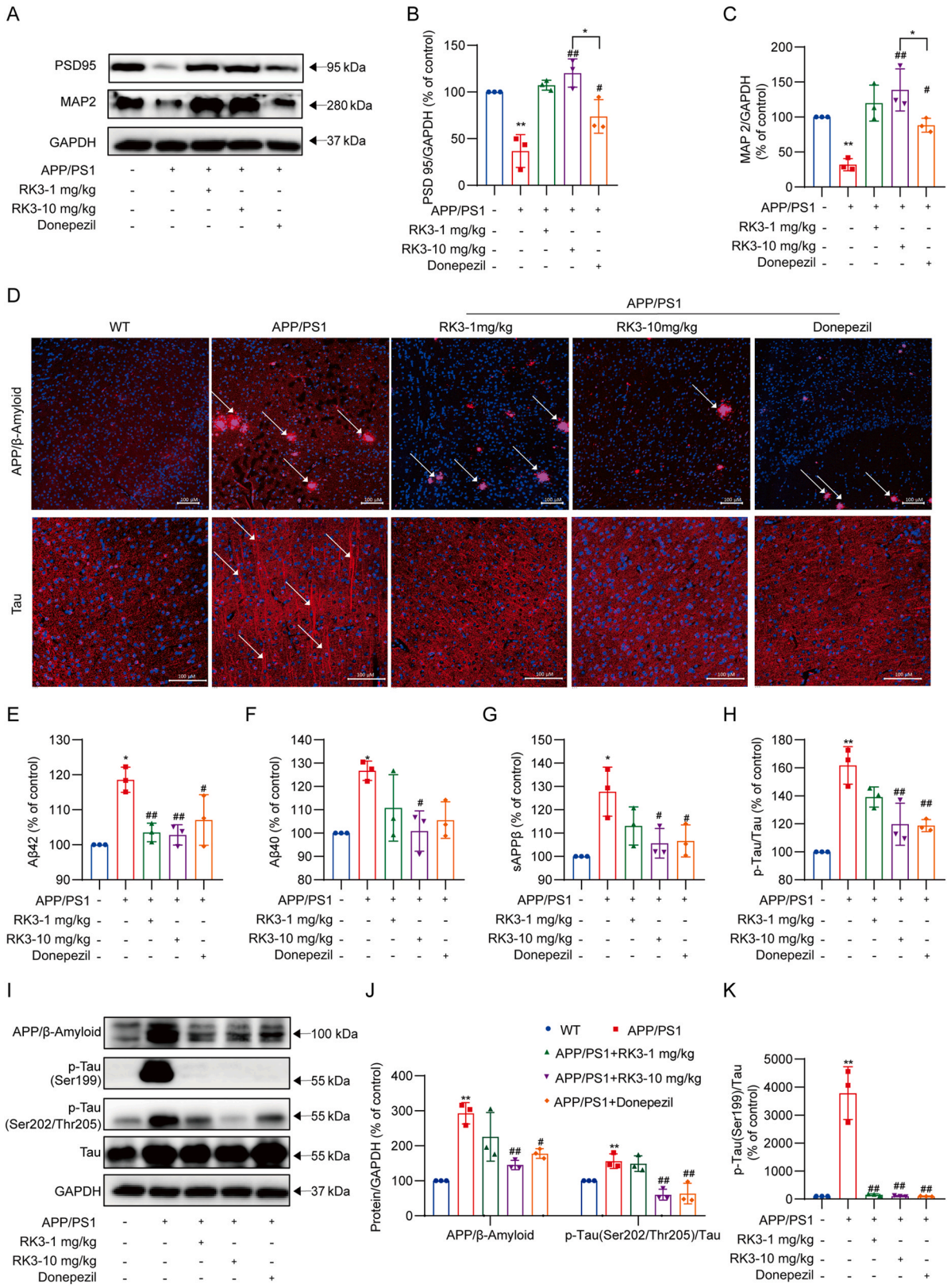

Fig. 5. Rk3 treatment reduced AD pathology of APP/PS1 mice. (A) Representative Western blot analysis of MAP2 and PSD95 in the hippocampus. GAPDH was used as the loading control. (B-C) Quantitative data of the blot intensity of corresponding proteins were determined by Image J software in-plane A. (D) Representative images of immunofluorescence in the hippocampus of 3 groups mice at 8 months old. Scale bar 100 μm. (E-H) Aβ42, Aβ40, sAPPβ, p-tau and tau levels in the hippocampus were determined using ELISA kits respectively. (I) Representative western blot analysis of APP, p-Tau (Ser199), p-Tau (Ser202/Thr205) and Tau in the hippocampus. GAPDH was used as the loading control. (J-K) Quantitative data of the blot intensity of corresponding proteins were determined by Image J software in-plane A. Results are presented as mean ± SEM (n = 3). *P < 0.05 or * *P < 0.01, or * **P < 0.001 versus the WT group; $^{\#}$P < 0.05 or $^{\#\#}$P < 0.01 versus the APP/PS1 group.

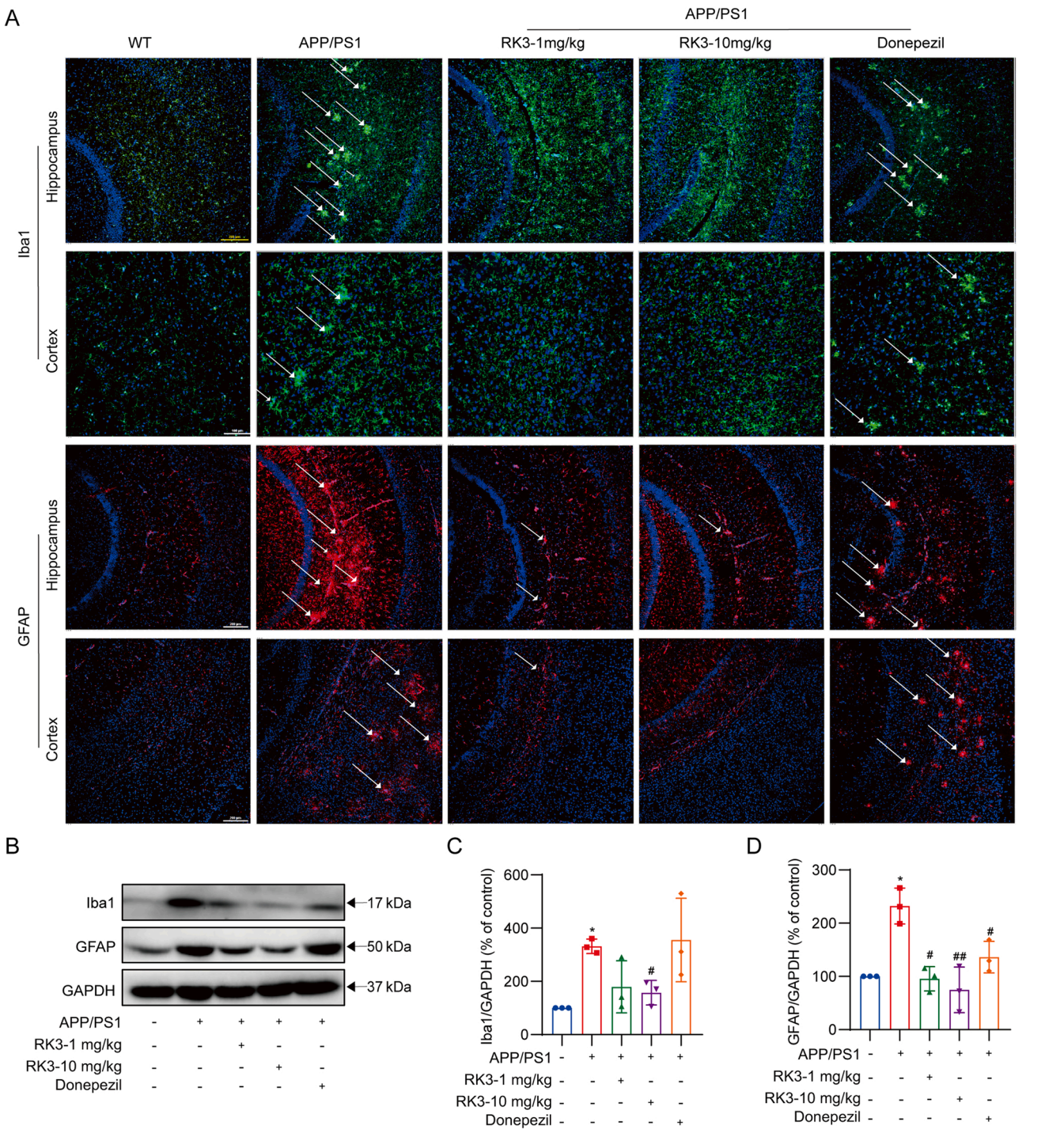

Fig. 6. Rk3 treatment reduced glia cell activation of APP/PS1 mice. (A) Representative images of Iba1 and GFAP staining in different brain regions. Scale bar 200 μm and 100 μm. (B) Representative western blot analysis of Iba1 and GFAP in the hippocampus. GAPDH was used as the loading control. (C-D) Quantitative data of the blot intensity of corresponding proteins were determined by Image J software in-plane A. Results are presented as mean ± SEM (n = 3). *P < 0.05 or * *P < 0.01, or * **P < 0.001 versus the WT group; $^{\#}$P < 0.05 or $^{\#\#}$P < 0.01 versus the APP/PS1 group.

enzymes, glutathione peroxidase (Gpx) family and NAD(P)H: quinone oxidoreductase 1 (NQO1). The Nrf2-driven free radical detoxification pathways are important endogenous homeostatic mechanisms [48]. In addition, it was reported that the cellular antioxidant system relies on the Nrf2 dissociation from Keap1 and its subsequent translocation to the nucleus, where the activation of antioxidant genes occurs [49]。In the present study, we found that Rk3 activates Nrf2 in Aβ-induced PC12 neuronal cultures and APP/PS1 mice, which is associated with antioxidant and neurotherapeutic effects. It illustrates that Rk3 is a good antioxidant, mitochondria is the main site of ROS production, and mitochondrial dysfunction caused by oxidative stress plays a key role in the pathogenesis of aging-related neurodegenerative diseases [50].

Mitochondria are the main site of ROS production, and mitochondrial dysfunction caused by oxidative stress plays a key role in the pathogenesis of aging-related neurodegenerative diseases [50]. We further found a protective effect of Rk3 on Δψm, mitochondria acting as energy factories in cells, producing most of the cellular ATP. Several studies have shown that ginsenosides protect neurons by reducing

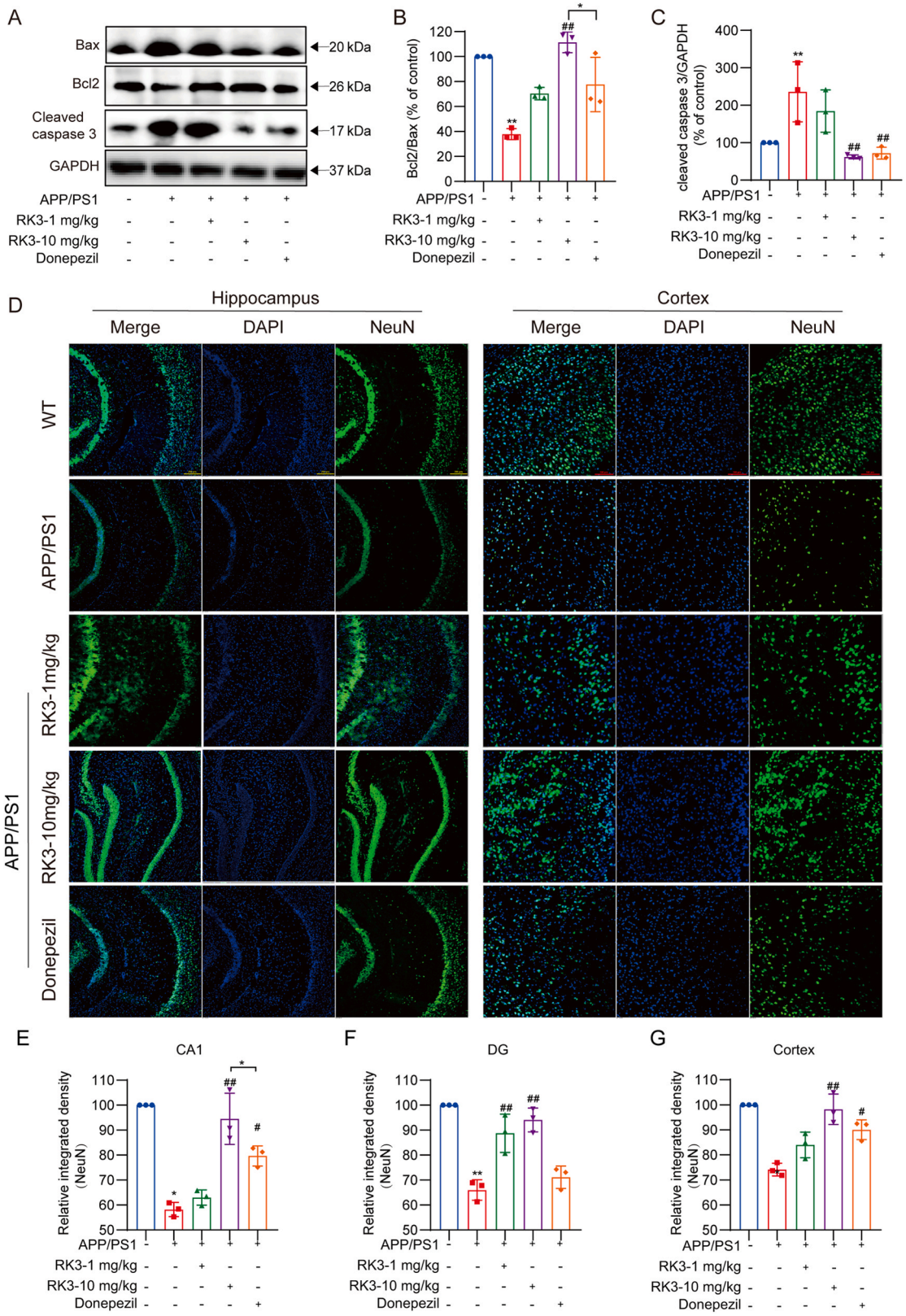

Fig. 7. Rk3 treatment reduced decreased neuron apoptosis of APP/PS1 mice. (A) Representative Western blot analysis of Bax, Bcl2 and Cleaved caspase3 in the hippocampus. GAPDH was used as the loading control. (B-C) Quantitative data of the blot intensity of corresponding proteins were determined by Image J software in-plane A. (D) Representative images of NeuN staining in different brain regions. (E-F) Quantification of NeuN cells in hippocampus CA1, DG and cortex with a NeuN antibody. Results are presented as mean ± SEM (n = 3). *P < 0.05 or * *P < 0.01, or * **P < 0.001 versus the WT group; #P < 0.05 or ##P < 0.01 versus the APP/PS1 group.

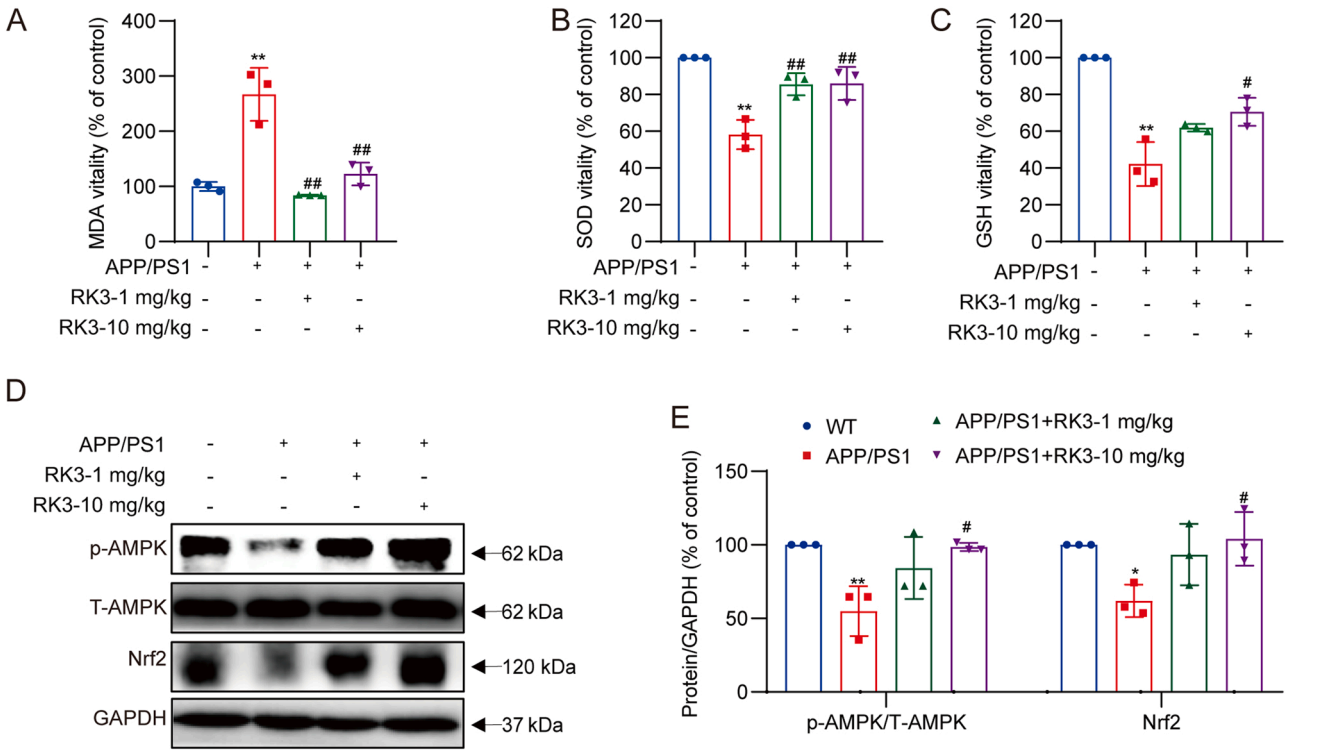

Fig. 8. Rk3 attenuated the histopathological changes in APP/PS1 mice by activation of AMPK. (A-C) MDA, SOD and GSH levels in the hippocampus were determined using biochemical kits respectively. (D) Representative Western blot analysis of p-AMPK and T-AMPK in the hippocampus. (E) Quantitative data of the blot intensity of corresponding proteins were determined by Image J software in-plane A. Results are presented as mean ± SEM (n = 3). *P < 0.05 or * *P < 0.01, or * **P < 0.001 versus the WT group; $^{\#}$P < 0.05 or $^{\#\#}$P < 0.01 versus the APP/PS1 group.

mitochondrial-mediated cell death [22]. AMPK constitutes another main metabolic supervisor in almost all cell lineages, and governs the energy status of the cell through sensing AMP/ATP, amino acid and glucose levels, and tracking mitochondrial conditions [51]. AMPK is known to phosphorylate Nrf2 at Ser550 residues and promote the nuclear accumulation of Nrf2 for ARE-driven gene transactivation that promotes cellular antioxidant capacity [52]. The role of AMPK in AD is not fully understood. Numerous studies have shown that Aβ impairs mitochondrial respiratory complex function and induces AMPK activity in AD [53]. Conversely, one study showed that oligomeric Aβ42 impaired AMPK phosphorylation to activate GSK3β and induce tau hyperphosphorylation in a fly model of AD [54]. The current findings suggest that Rk3 can activate the AMPK-Nrf2 pathway in vitro and in vivo. And found that compound C blocked the effect of Rk3 on AMPK activation in Aβ-induced PC12 and primary neuronal cells, thereby blocking the protective effect of Rk3, further proved that Rk3 produces antioxidant effect and neuroprotection through AMPK-Nrf2 effect.

The current research on Rk3 is still limited, the bioavailability and pharmacokinetics of Rk3 are less studied. And our study was limited to explain how Rk3 activate AMPK signaling pathway. However, at least our findings provide preliminary evidence for the positive effects of AMPK activation on Aβ and related pathologies in APP/PS1 mice.

In conclusion, Rk3 attenuates Aβ-induced neuronal injury accompanied by activating the AMPK pathway and promoting the expression of Nrf2 and its target genes *Ho-1*, *Nqo1* and *keap1*. Inhibition of the AMPK pathway reduces the protective effect of RK3. Similarly, Rk3 effectively attenuated cognitive impairment and pathology in APP/PS1 mice. Importantly, the therapeutic effect of Rk3 was better than the positive drug donepezil. Taken together, the results of this study support ginsenoside Rk3 as a new strategy for AD treatment.

Author contributions

Guang Liang, Xia Zhao and Wei Wang contributed to the literature search and study design. Lingyu She participated in the drafting of the article. Guang Liang and Xia Zhao contribute to manuscript modification. Lingyu She, Li Xiong, Weili Li, Jing Zhang, Jinfeng Sun, Juan Ren, Haibin Wu carried out the experiments.

CRediT authorship contribution statement

Guang Liang, Xia Zhao and Wei Wang contributed to the literature search and study design. Lingyu She participated in the drafting of the article. Guang Liang and Xia Zhao contribute to manuscript modification. Lingyu She, Li Xiong, Weili Li, Jing zhang, Jinfeng Sun, Juan Ren, Haibin Wu carried out the experiments. All authors have read and approved the final manuscript. All authors contributed to data analysis, drafting or revising the article, agreed on the journal to which the article will be submitted, gave final approval of the version to be published, and agreed to be accountable for all aspects of the work.

Conflict of interest statement

The authors have no conflicts of interest to declare.

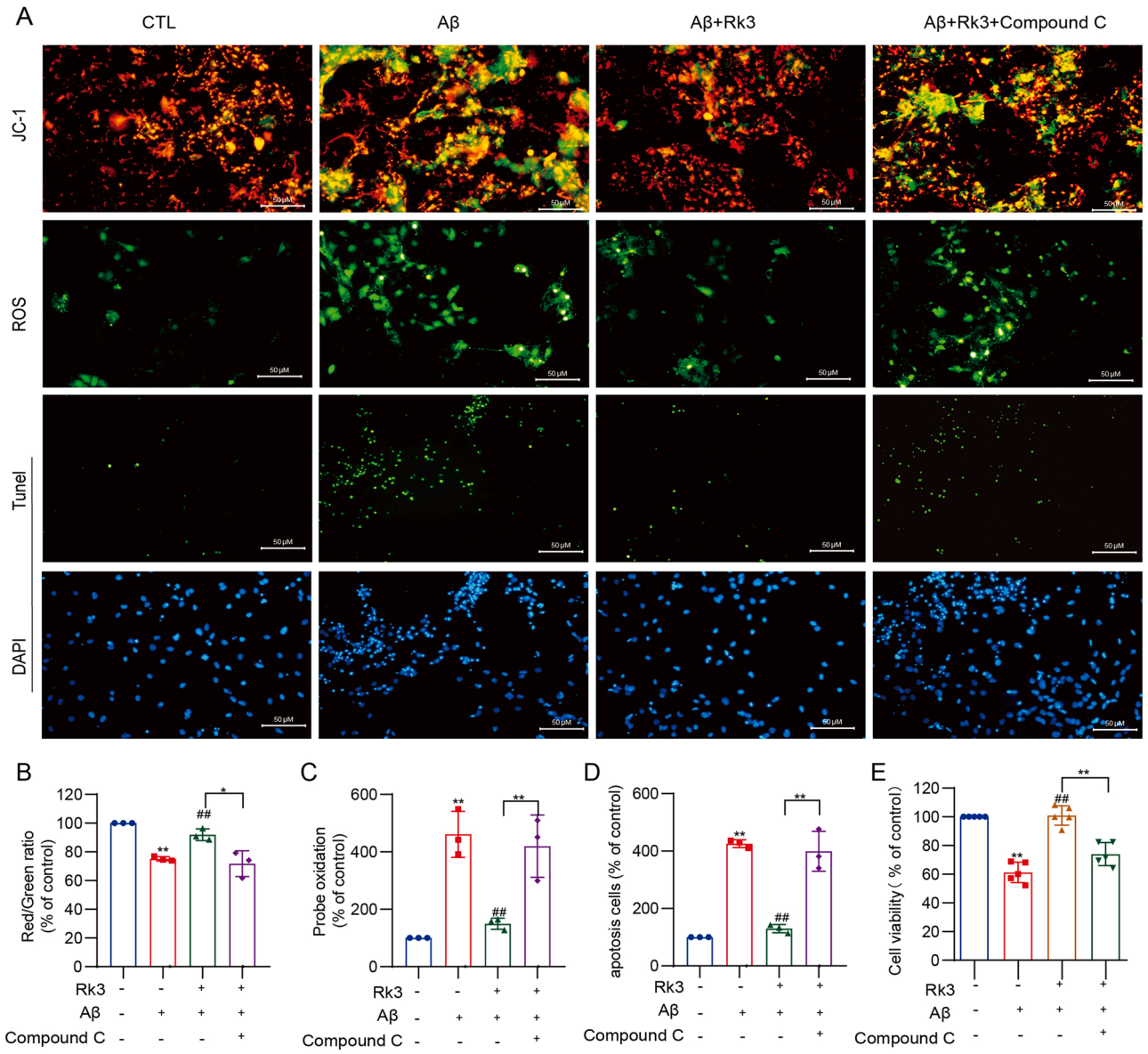

Fig. 9. Rk3 conferred neuroprotective effect on Aβ induced in neuronal cells. Neuronal cells were pretreated with or without the presence of 2 μM compound C. After 30 min, neuronal cells are used 10 μM Rk3 for 24 h. Then, cells were exposed to 10 μM Aβ for 24 h. (A) Determined mitochondrial membrane potential by staining the cells with JC-1 dyes, the fluorescent images represent the ROS level as determined by the probes DCFH-DA, and TUNEL staining. (B) Red to green fluorescence intensity ratio (increase of mitochondrial membrane potential). (C) Quantitation of the percentage of the cellular ROS level. (D) Quantitation of TUNEL staining data. (E) Cell viability was measured using the MTT assay. Results are presented as mean ± SEM (n = 3). *P < 0.05 or * *P < 0.01, or * **P < 0.001, CTL vs Aβ; $^{\#}$P < 0.05 or $^{\#\#}$P < 0.01 Aβ vs Aβ+ Rk3.

Data Availability

Data will be made available on request.

Acknowledgments

This study was supported by Zhejiang Provincial Key Scientific Project (2021C03041 to G.L.) and Hangzhou Medical College (00004F1RCYJ2109 to X.Z.).

Appendix A. Supporting information

Supplementary data associated with this article can be found in the online version at doi:10.1016/j.biopha.2022.114192.

References

[1] P. Scheltens, K. Blennow, M.M.B. Breteler, B. de Strooper, G.B. Frisoni, S. Salloway, W.M. Van der Flier, Alzheimer's disease, Lancet (Lond., Engl.) 388 (2016) 505–517, https://doi.org/10.1016/S0140-6736(15)01124-1.
[2] H.W. Querfurth, F.M. LaFerla, Alzheimer's disease, N. Engl. J. Med. 362 (2010) 329–344, https://doi.org/10.1056/NEJMRA0909142.
[3] Z. Wang, Q. Xu, F. Cai, X. Liu, Y. Wu, W. Song, BACE2, a conditional β-secretase, contributes to Alzheimer's disease pathogenesis, JCI Insight 4 (2019), https://doi.org/10.1172/JCI.INSIGHT.123431.
[4] A.E. Behar, L. Sabater, M. Baskin, C. Hureau, G. Maayan, A. Water-Soluble Peptoid Chelator, Water-soluble peptoid chelator that can remove cu 2+ from amyloid-β peptides and stop the formation of reactive oxygen species associated with Alzheimer's diseasee, Angew. Chem. Int. Ed. Engl. 60 (2021) 24588–24597, https://doi.org/10.1002/ANIE.202109758.
[5] R. Bai, J. Guo, X.Y. Ye, Y. Xie, T. Xie, Oxidative stress: the core pathogenesis and mechanism of Alzheimer's disease, Ageing Res. Rev. 77 (2022), 101619, https://doi.org/10.1016/J.ARR.2022.101619.
[6] T. Saito, S. Hisahara, N. Iwahara, M.C. Emoto, K. Yokokawa, H. Suzuki, T. Manabe, A. Matsumura, S. Suzuki, T. Matsushita, J. Kawamata, H. Sato-Akaba, H.G. Fujii,

S. Shimohama, Early administration of galantamine from preplaque phase suppresses oxidative stress and improves cognitive behavior in APPswe/PS1dE9 mouse model of Alzheimer's disease, Free Radic. Biol. Med. 145 (2019) 20–32, https://doi.org/10.1016/J.FREERADBIOMED.2019.09.014.
[7] S.C. Lin, D.G. Hardie, AMPK: sensing glucose as well as cellular energy status, Cell Metab. 27 (2018) 299–313, https://doi.org/10.1016/J.CMET.2017.10.009.
[8] D.A. Butterfield, B. Halliwell, Oxidative stress, dysfunctional glucose metabolism and Alzheimer disease, Nat. Rev. Neurosci. 20 (2019) 148–160, https://doi.org/10.1038/S41583-019-0132-6.
[9] Q. Zheng, B. Song, G. Li, F. Cai, M. Wu, Y. Zhao, L.L. Jiang, T. Guo, M. Shen, H. Hou, Y. Zhou, Y. Zhao, A. Di, L. Zhang, F. Zeng, X.F. Zhang, H. Luo, X. Zhang, H. Zhang, Z. Zeng, T.Y. Huang, C. Dong, H. Qing, Y. Zhang, Q. Zhang, X. Wang, Y. Wu, H. Xu, W. Song, X. Wang, USP25 inhibition ameliorates Alzheimer's pathology through the regulation of APP processing and Aβ generation, J. Clin. Invest 132 (2022), https://doi.org/10.1172/JCI152170.
[10] L. Wang, J. Han, P. Shan, S. You, X. Chen, Y. Jin, J. Wang, W. Huang, Y. Wang, G. Liang, MD2 blockage protects obesity-induced vascular remodeling via activating AMPK/Nrf2, Obes. (Silver Spring) 25 (2017) 1532–1539, https://doi.org/10.1002/OBY.21916.
[11] Y. Zhang, X. Yang, S. Wang, S. Song, Ginsenoside Rg3 prevents cognitive impairment by improving mitochondrial dysfunction in the rat model of Alzheimer's Disease, J. Agric. Food Chem. 67 (2019) 10048–10058, https://doi.org/10.1021/ACS.JAFC.9B03793.
[12] B. Zhao, C. Lv, J. Lu, Natural occurring polysaccharides from Panax ginseng C. A. Meyer: a review of isolation, structures, and bioactivities, Int. J. Biol. Macromol. 133 (2019) 324–336, https://doi.org/10.1016/j.ijbiomac.2019.03.229.
[13] H. Zhang, Y. Su, Z. Sun, M. Chen, Y. Han, Y. Li, X. Dong, S. Ding, Z. Fang, W. Li, W. Li, Ginsenoside Rg1 alleviates Aβ deposition by inhibiting NADPH oxidase 2 activation in APP/PS1 mice, J. Ginseng Res. 45 (2021) 665, https://doi.org/10.1016/J.JGR.2021.03.003.
[14] J. jiao Wu, Y. Yang, Y. Wan, J. Xia, J.F. Xu, L. Zhang, D. Liu, L. Chen, F. Tang, H. Ao, C. Peng, New insights into the role and mechanisms of ginsenoside Rg1 in the management of Alzheimer's disease, Biomed. Pharmacother. 152 (2022), https://doi.org/10.1016/J.BIOPHA.2022.113207.
[15] A. Rajabian, M. Rameshrad, H. Hosseinzadeh, Therapeutic potential of Panax ginseng and its constituents, ginsenosides and gintonin, in neurological and neurodegenerative disorders: a patent review, Expert Opin. Ther. Pat. 29 (2019) 55–72, https://doi.org/10.1080/13543776.2019.1556258.
[16] J. Li, Q. Huang, J. Chen, H. Qi, J. Liu, Z. Chen, D. Zhao, Z. Wang, X. Li, Neuroprotective potentials of panax ginseng against Alzheimer's disease: a review of preclinical and clinical evidences, Front. Pharm. 12 (2021), https://doi.org/10.3389/FPHAR.2021.688490.
[17] H.J. Kim, S.W. Jung, S.Y. Kim, I.H. Cho, H.C. Kim, H. Rhim, M. Kim, S.Y. Nah, Panax ginseng as an adjuvant treatment for Alzheimer's disease, J. Ginseng Res. 42 (2018) 401–411, https://doi.org/10.1016/J.JGR.2017.12.008.
[18] X. Bai, R. Fu, Z. Duan, P. Wang, C. Zhu, D. Fan, Ginsenoside Rk3 alleviates gut microbiota dysbiosis and colonic inflammation in antibiotic-treated mice, Food Res. Int. 146 (2021), https://doi.org/10.1016/J.FOODRES.2021.110465.
[19] S.H. Baek, B.K. Shin, N.J. Kim, S.Y. Chang, J.H. Park, Protective effect of ginsenosides Rk3 and Rh4 on cisplatin-induced acute kidney injury in vitro and in vivo, J. Ginseng Res. 41 (2017) 233–239, https://doi.org/10.1016/J.JGR.2016.03.008.
[20] R.L. Richardson, E.M. Kim, R.A. Shephard, T. Gardiner, J. Cleary, E. O'Hare, Behavioural and histopathological analyses of ibuprofen treatment on the effect of aggregated Aβ(1-42) injections in the rat, Brain Res 954 (2002) 1–10, https://doi.org/10.1016/S0006-8993(02)03006-8.
[21] Z. Hruska, G.P. Dohanich, The effects of chronic estradiol treatment on working memory deficits induced by combined infusion of beta-amyloid (1-42) and ibotenic acid, Horm. Behav. 52 (2007) 297–306, https://doi.org/10.1016/J.YHBEH.2007.05.010.
[22] M. Liu, X. Bai, S. Yu, W. Zhao, J. Qiao, Y. Liu, D. Zhao, J. Wang, S. Wang, Ginsenoside re inhibits ROS/ASK-1 dependent mitochondrial apoptosis pathway and activation of Nrf2-antioxidant response in beta-amyloid-challenged SH-SY5Y cells, Molecules 24 (2019), https://doi.org/10.3390/MOLECULES24152687.
[23] X. Zhao, X. Huang, C. Yang, Y. Jiang, W. Zhou, W. Zheng, Artemisinin Attenuates Amyloid-Induced Brain Inflammation and Memory Impairments by Modulating TLR4/NF-κB Signaling, Int. J. Mol. Sci. 23 (2022), https://doi.org/10.3390/IJMS23116354.
[24] R.M. Friedlander, Apoptosis and caspases in neurodegenerative diseases, N. Engl. J. Med. 348 (2003) 1365–1375, https://doi.org/10.1056/NEJMRA022366.
[25] J. Han, J. Xia, L. Zhang, E. Cai, Y. Zhao, X. Fei, X. Jia, H. Yang, S. Liu, Studies of the effects and mechanisms of ginsenoside Re and Rk3 on myelosuppression induced by cyclophosphamide, J. Ginseng Res. 43 (2019) 618–624, https://doi.org/10.1016/J.JGR.2018.07.009.
[26] C. Zang, H. Liu, J. Shang, H. Yang, L. Wang, C. Sheng, Z. Zhang, X. Bao, Y. Yu, X. Yao, D. Zhang, Gardenia jasminoides J.Ellis extract GJ-4 alleviated cognitive deficits of APP/PS1 transgenic mice, Phytomedicine 93 (2021), https://doi.org/10.1016/J.PHYMED.2021.153780.
[27] S. Li, X. Zhao, P. Lazarovici, W. Zheng, Artemether activation of AMPK/GSK3 β(ser9)/Nrf2 signaling confers neuroprotection towards β- amyloid-induced neurotoxicity in 3xTg Alzheimer's mouse model, Oxid. Med. Cell. Longev. (2019) (2019), https://doi.org/10.1155/2019/1862437.
[28] T.-J. Lyu, Z.-X. Zhang, J. Chen, Z.-J. Liu, Ginsenoside Rg1 ameliorates apoptosis, senescence and oxidative stress in ox-LDL-induced vascular endothelial cells via the AMPK/SIRT3/p53 signaling pathway, Exp. Ther. Med. 24 (2022) 1–10, https://doi.org/10.3892/ETM.2022.11482.
[29] L. Fão, S.I. Mota, A.C. Rego, Shaping the Nrf2-ARE-related pathways in Alzheimer's and Parkinson's diseases, Ageing Res. Rev. 54 (2019), https://doi.org/10.1016/J.ARR.2019.100942.
[30] J.S. Park, Y.Y. Lee, J. Kim, H. Seo, H.S. Kim, β-Lapachone increases phase II antioxidant enzyme expression via NQO1-AMPK/PI3K-Nrf2/ARE signaling in rat primary astrocytes, Free Radic. Biol. Med. 97 (2016) 168–178, https://doi.org/10.1016/J.FREERADBIOMED.2016.05.024.
[31] M. Garcia-Alloza, E.M. Robbins, S.X. Zhang-Nunes, S.M. Purcell, R.A. Betensky, S. Raju, C. Prada, S.M. Greenberg, B.J. Bacskai, M.P. Frosch, Characterization of amyloid deposition in the APPswe/PS1dE9 mouse model of Alzheimer disease, Neurobiol. Dis. 24 (2006) 516–524, https://doi.org/10.1016/J.NBD.2006.08.017.
[32] I.A. Kuznetsov, A.V. Kuznetsov, How the formation of amyloid plaques and neurofibrillary tangles may be related: a mathematical modelling study, Proc. Math. Phys. Eng. Sci. 474 (2018), https://doi.org/10.1098/RSPA.2017.0777.
[33] M. Zhao, X.F. Jiang, H.Q. Zhang, J.H. Sun, H. Pei, L.N. Ma, Y. Cao, H. Li, Interactions between glial cells and the blood-brain barrier and their role in Alzheimer's disease, Ageing Res. Rev. 72 (2021), https://doi.org/10.1016/J.ARR.2021.101483.
[34] P. Gao, Z. Wang, M. Lei, J. Che, S. Zhang, T. Zhang, Y. Hu, L. Shi, L. Cui, J. Liu, M. Noda, Y. Peng, J. Long, Daphnetin ameliorates Aβ pathogenesis via STAT3/GFAP signaling in an APP/PS1 double-transgenic mouse model of Alzheimer's disease, Pharmacol. Res. 180 (2022), 106227, https://doi.org/10.1016/J.PHRS.2022.106227.
[35] F. Jie, X. Yang, B. Yang, Y. Liu, L. Wu, B. Lu, Stigmasterol attenuates inflammatory response of microglia via NF-κB and NLRP3 signaling by AMPK activation, Biomed. Pharmacother. 153 (2022), 113317, https://doi.org/10.1016/J.BIOPHA.2022.113317.
[36] B. Mazur-Kolecka, D. Kowal, T. Sukontasup, D. Dickson, J. Frackowiak, The effect of oxidative stress on amyloid precursor protein processing in cells engaged in beta-amyloidosis is related to apolipoprotein E genotype, Acta Neuropathol. 108 (2004) 287–294, https://doi.org/10.1007/S00401-004-0890-7.
[37] S. Piatnitskaia, M. Takahashi, H. Kitaura, Y. Katsuragi, T. Kakihana, L. Zhang, A. Kakita, Y. Iwakura, H. Nawa, T. Miura, T. Ikeuchi, T. Hara, M. Fujii, USP10 is a critical factor for Tau-positive stress granule formation in neuronal cells, 2019 91, Sci. Rep. 9 (2019) 1–15, https://doi.org/10.1038/s41598-019-47033-7.
[38] A. Dey, R. Bhattacharya, A. Mukherjee, D.K. Pandey, Natural products against Alzheimer's disease: Pharmaco-therapeutics and biotechnological interventions, Biotechnol. Adv. 35 (2017) 178–216, https://doi.org/10.1016/J.BIOTECHADV.2016.12.005.
[39] H. Liu, X. Lu, Y. Hu, X. Fan, Chemical constituents of Panax ginseng and Panax notoginseng explain why they differ in therapeutic efficacy, Pharmacol. Res. 161 (2020), https://doi.org/10.1016/J.PHRS.2020.105263.
[40] G. Cao, P. Su, S. Zhang, L. Guo, H. Zhang, Y. Liang, C. Qin, W. Zhang, Ginsenoside Re reduces Aβ production by activating PPARγ to inhibit BACE1 in N2a/APP695 cells, Eur. J. Pharmacol. 793 (2016) 101–108, https://doi.org/10.1016/J.EJPHAR.2016.11.006.
[41] X. Yan, G. Hu, W. Yan, T. Chen, F. Yang, X. Zhang, G. Zhao, J. Liu, Ginsenoside Rd promotes non-amyloidogenic pathway of amyloid precursor protein processing by regulating phosphorylation of estrogen receptor alpha, Life Sci. 168 (2017) 16–23, https://doi.org/10.1016/J.LFS.2016.11.002.
[42] F. Fang, X. Chen, T. Huang, L.F. Lue, J.S. Luddy, S.S.Du Yan, Multi-faced neuroprotective effects of Ginsenoside Rg1 in an Alzheimer mouse model, Biochim. Biophys. Acta 2012 (1822) 286, https://doi.org/10.1016/J.BBADIS.2011.10.004.
[43] C. Shi, D.D. Zheng, L. Fang, F. Wu, W.H. Kwong, J. Xu, Ginsenoside Rg1 promotes nonamyloidgenic cleavage of APP via estrogen receptor signaling to MAPK/ERK and PI3K/Akt, Biochim. Biophys. Acta 1820 (2012) 453–460, https://doi.org/10.1016/J.BBAGEN.2011.12.005.
[44] J. Qiu, W. Li, S.H. Feng, M. Wang, Z.Y. He, Ginsenoside Rh2 promotes nonamyloidgenic cleavage of amyloid precursor protein via a cholesterol-dependent pathway, Genet. Mol. Res. 13 (2014) 3586–3598, https://doi.org/10.4238/2014.MAY.9.2.
[45] L. Li, J. Liu, X. Yan, K. Qin, M. Shi, T. Lin, Y. Zhu, T. Kang, G. Zhao, Protective effects of ginsenoside Rd against okadaic acid-induced neurotoxicity in vivo and in vitro, J. Ethnopharmacol. 138 (2011) 135–141, https://doi.org/10.1016/J.JEP.2011.08.068.
[46] L. Qu, R. Fu, X. Ma, D. Fan, Hepatoprotective effects of ginsenoside Rk3 in acetaminophen-induced liver injury in mice by activation of autophagy, Food Funct. 12 (2021) 9128–9140, https://doi.org/10.1039/D1FO02081A.
[47] Y. Yang, X. Liang, P. Jin, N. Li, Q. Zhang, W. Yan, H. Zhang, J. Sun, Screening and determination for potential acetylcholinesterase inhibitory constituents from ginseng stem-leaf saponins using ultrafiltration (UF)-LC-ESI-MS 2, Phytochem. Anal. 30 (2019) 26–33, https://doi.org/10.1002/PCA.2787.
[48] A. Osama, J. Zhang, J. Yao, X. Yao, J. Fang, Nrf2: a dark horse in Alzheimer's disease treatment, Ageing Res. Rev. 64 (2020), https://doi.org/10.1016/J.ARR.2020.101206.
[49] M. Kobayashi, M. Yamamoto, Molecular mechanisms activating the Nrf2-Keap1 pathway of antioxidant gene regulation, Antioxid. Redox Signal. 7 (2005) 385–394, https://doi.org/10.1089/ARS.2005.7.385.
[50] M. Golpich, E. Amini, Z. Mohamed, R. Azman Ali, N. Mohamed Ibrahim, A. Ahmadiani, Mitochondrial dysfunction and biogenesis in neurodegenerative diseases: pathogenesis and treatment, CNS Neurosci. Ther. 23 (2017) 5, https://doi.org/10.1111/CNS.12655.
[51] I. Benito-Cuesta, L. Ordóñez-Gutiérrez, F. Wandosell, AMPK activation does not enhance autophagy in neurons in contrast to MTORC1 inhibition: different impact on β-amyloid clearance, Autophagy 17 (2021) 656, https://doi.org/10.1080/15548627.2020.1728095.

[52] J. Duan, J. Cui, Z. Yang, C. Guo, J. Cao, M. Xi, Y. Weng, Y. Yin, Y. Wang, G. Wei, B. Qiao, A. Wen, Neuroprotective effect of Apelin 13 on ischemic stroke by activating AMPK/GSK-3β/Nrf2 signaling, J. Neuroinflamm. 16 (2019), https://doi.org/10.1186/S12974-019-1406-7.

[53] L. Yang, Y. Jiang, L. Shi, D. Zhong, Y. Li, J. Li, R. Jin, AMPK: potential therapeutic target for Alzheimer's disease, Curr. Protein Pept. Sci. 21 (2020) 66–77, https://doi.org/10.2174/1389203720666190819142746.

[54] H. Park, T.I. Kam, Y. Kim, H. Choi, Y. Gwon, C. Kim, J.Y. Koh, Y.K. Jung, Neuropathogenic role of adenylate kinase-1 in Aβ-mediated tau phosphorylation via AMPK and GSK3β, Hum. Mol. Genet 21 (2012) 2725–2737, https://doi.org/10.1093/HMG/DDS100.